Photoelectron Spectroscopy of Silver and Palladium Cluster Anions

Electron Delocalization *versus* Localization

G. Ganteför, M. Gausa, K-H. Meiwes-Broer* and H. O. Lutz
Fakultät für Physik, Universität Bielefeld, 4800 Bielefeld 1, Federal Republic of Germany

Photoelectrons (PE) from jet-cooled mass-identified silver and palladium cluster anions (number of atoms, $n \leqslant 21$) were detached by UV laser light and energy-analysed in a time-of-flight (TOF) electron spectrometer of the magnetic-bottle type. For palladium PE threshold energies smoothly increase with n; for Ag, they show clear evidence of shell effects as well as an 'even–odd oscillation'. The PE energy spectra are strongly structured, the structures being attributed to transitions involving the neutral ground states as well as contributions of low-lying excited neutral states. For silver the results can, in part, be qualitatively understood in terms of a delocalized electron Fermi-gas within the ellipsoidal deformed cluster. This picture fails for the more localized d electrons of palladium. For a thorough interpretation more elaborate calculations are necessary. The first results are available for alkali-metal clusters and will be compared to the silver and copper data.

The confinement of a (nearly) free fermion gas gives rise to discrete energy levels. The order and spacing of the levels depend on the geometry of the confined volume as well as the details of the effective potential seen by the electrons. Such 'quantum size' effects are well known from, *e.g.*, nuclear physics; they are expected to play an important role in the transition regime between atom and solid-state physics.

From recent work it has become evident that gas-phase metal clusters are well suited to model such confined systems: Early evidence has come, in particular, from the study of abundances in beams of ionized clusters which showed structures reminiscent of the nuclear physics 'magic numbers'. The assumption of a delocalized electron gas, confined to the dimensions of the cluster ['jellium model', *cf.* ref. (1)–(3)] has proven to be especially suited to explain the behaviour of Group Ia, b elements. Quantum-chemical or molecular dynamics calculations considering also the exact geometrical cluster structures yielded results mainly on ground-state binding energies, ionization potentials and electron affinities.[4–11] Only recently, however, has the development of intense cluster-ion beams and their subsequent mass analysis allowed the application of the powerful technique of photo-electron (PE) spectroscopy to clusters of a defined mass,[12–19] thereby allowing a deeper insight into the electronic level structure of these systems.

In this paper we present a study of photoelectrons involving and comparing two very different cluster systems with (*a*) rather delocalized (Ag_n^-) and (*b*) rather localized (Pd_n^-) valence electrons. For Ag_n^- it is found that a varying cluster size, n, has a dramatic influence on the PE energy spectra. In this case, the jellium model provides an at least qualitative explanation of some features of electron-state density mapping provided by the technique of PE spectroscopy. In addition, recent investigations on alkali-metal clusters with the quantum-chemical CI procedure by Koutecký *et al.*[20] give hope that soon a rather detailed understanding of cluster level structure might also be developed for larger systems. In contrast, Pd_n^- cluster PE spectra depend only weakly on cluster size, n, in agreement with what might be expected for the more localized d valence electrons.

Experimental

Our experimental method has been described elsewhere.[18,21,22] In short, laser vaporization of a target rod of the desired metal mounted in a pulsed, high-pressure supersonic nozzle[23,24] is used. Pulsed excimer laser light (*ca.* 100 mJ per pulse) produces an intense plasma which is flushed by a carrier gas pulse through a channel into high vacuum. As the source chamber is carefully kept free of electric fields the supersonic jet contains positive and negative cluster ions when it enters the TOF mass spectrometer behind the skimmer. After pulsed acceleration collinearly in the source direction the ions are spatially and temporally focused into the starting area of a TOF electron spectrometer of the 'magnetic bottle'[25] type. A second pulsed UV laser is fired at a selected cluster bunch which (by its drift time) has been mass selected. One bunch contains typically between 10 and 10^3 cluster ions as estimated from the channeltron response.

Kruit *et al.*[25] have shown that electrons need nearly the same flight time independent of their emission angles if they are born in a strong magnetic field and subsequently guided by a weak field to the detector. A 4π steradian acceptance is theoretically possible. Our spectrometer is based on this idea; the high field (*ca.* 140 mT in the detachment zone) is produced by an electromagnet with an iron core, the guiding field (0.5–1 mT) is created by a 2 m long coil within a μ-metal shield. From an intense anion bunch up to *ca.* 10 photoelectrons per laser shot may be detected. However, under normal operation the power of the detaching laser is reduced in order to avoid multiphoton ionization of anions or the residual gas. Therefore, typical photoelectron currents are 0.1–1 electron per shot at a repetition rate of *ca.* 80 Hz.

The intrinsic energy resolution $\Delta E/E$ of a magnetic bottle electron spectrometer is roughly given by the magnetic field ratio.[25] Further limitation to $\Delta E/E$ arises from off-axis ionization; in addition, a non-isotropic electron emission angle (caused, *e.g.* by the laser polarization) may change the peak shape. Furthermore, we find a strong influence of anion velocity upon energy resolution (Doppler effect). To compensate for this effect the cluster ion energy has to be kept as low as possible. If necessary (particularly for light clusters) our collinear arrangement allows operation at ion beam energies below 20 eV;† no deceleration device is needed. The photoelectron spectra presented here are recorded at $\Delta E/E < 0.06$. The energy scale is calibrated by PE emission from Cu^- and Ag^- at different laser wavelengths, using the electron affinity, E_{ea}, values of the literature.[26] Fig. 1 shows as an example the Ag^- photodetachment line at an ion beam energy of 30 eV resolved with $\Delta E_{f.w.h.m.} \approx 80$ meV. No background correction or smoothing has been performed.

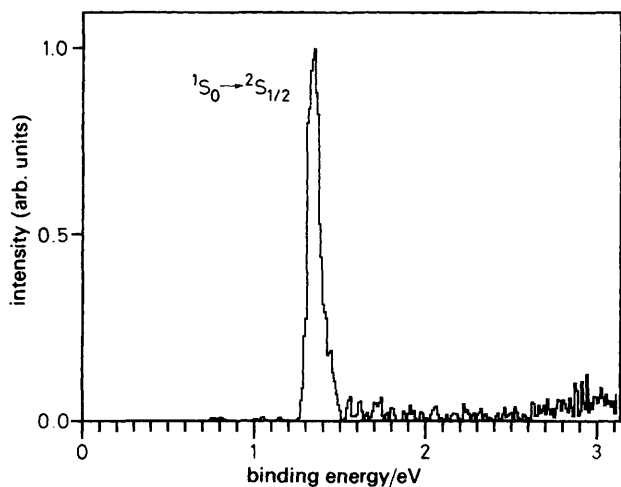† 1 eV = 1.602×10^{-19} J.

Fig. 1. Photoelectron calibration spectrum of Ag_1^- at a beam energy of 30 eV.

Results

Fig. 2 shows Ag_n^- and Pd_n^- mass spectra at a beam energy of 300 eV. With the exception of a few contaminants, mainly pure metal cluster anions are detected. In both spectra broad intensity distributions without significant steps or outstanding lines are measured. This behaviour is quite general for all positive and negative metal clusters produced by this source which have been studied so far.[17,18,21,22] In terms of cluster aggregation theory[27] our results imply that these systems belong to the diffusion-limited regime of aggregation kinetics in which the growth process occurs with a sticking coefficient
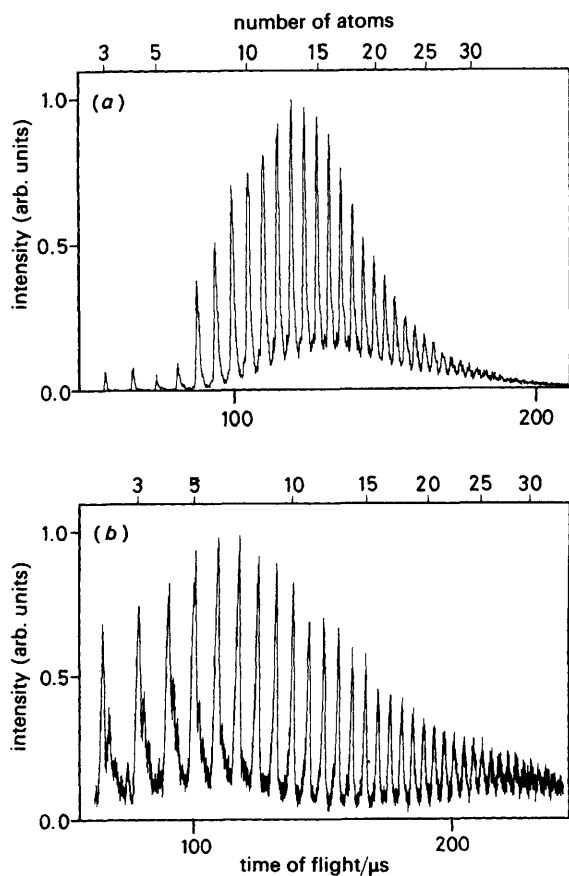

Fig. 2. TOF mass spectra of silver (a) and palladium (b) cluster anions, produced directly (i.e. without additional ionization) in a laser vaporization source. The ion bunches have an energy of 300 eV and are formed by grid switching.

of approximately unity. The heat of condensation is removed by the seeding gas and not by atom evaporation. Therefore, the cluster dissociation energies have only a minor influence upon the ion intensity distributions.

Pulsed UV laser light ($hv = 3.68$ and 5.0 eV, ≈ 0.5 mJ per pulse) is utilized to detach electrons from mass-identified anion bunches. In fig. 3 we present the PE spectra of Ag_n^- cluster anions in the size range 3–21 atoms, in fig. 4 those of Pd_n^-, $n = 2$–21. The data are plotted as a function of electron binding energy, i.e. the photon energy minus the kinetic energy of the detached electrons. The vertical axis represents full-scale photoelectron count (uncorrected for spectrometer efficiency etc.) so that the intensities do not directly represent the detachment cross-sections.

As a first result the PE spectra provide photodetachment threshold energies E_{TH} (marked by bars) as estimates of the upper bounds of adiabatic electron affinity (E_{ea}). Thresholds are arbitrarily taken as the onset of the electron signal above background (fixed at 1% of maximum intensity) corrected for instrumental broadening. Several electron spectra show broad threshold behaviour so that threshold energy determination depends more on intensity considerations than on instrumental resolution. Therefore, the onset uncertainties vary with cluster size as marked by the bar widths and as indicated in table 1.

Multiphoton effects and/or secondary effects such as photoneutralization of photofragments can be excluded as all features remain unchanged when the laser light flux is changed by a factor of ten. At present, more elaborate methods of threshold determination are not useful as the physical origin of the threshold shapes is unclear. In particular, if there is no distinct maximum in the spectrum, any threshold determination will, to a large extent, depend on the accumulated number of counts and will, therefore, be fairly arbitrary (cf. Pd_n^-, $n > 14$).

In fig. 3 and 4 the positions of the first strong peaks E_{MAX} are marked (with arrows). Only distinct peaks with more than 5% of the full maximum intensity are taken into consideration. We interpret the low-energy PE peaks as arising from vertical transitions involving final neutral ground states, i.e. the cluster undergoes no change in geometry upon ionization. In addition, several spectra contain peaks at higher binding energies, i.e. contributions arising from final excited neutral cluster states. Note that these states are probed in the geometry of the anions (vertical transitions), therefore the peak positions might be shifted relative to the term values of the neutrals. The energy differences between the first and the second peaks in some Ag_n^- PE energy spectra are also marked in fig. 3. These gaps can be related to the first excitation energies of the neutrals with the anion ground-state geometry and are equivalent in this picture to the so-called HOMO–LUMO gaps (energy differences between highest occupied and lowest unoccupied molecular orbitals).

The tabulated E_{TH} values are also displayed in fig. 5 as a function of cluster size. In the case of Ag_n^-, E_{TH} shows strong fluctuations for small n, superimposed on a slow rise to ca. 2.2 eV ($n = 19$). A pronounced drop appears at Ag_{20}^-. All values are far below the silver work function value of 4.26 eV.[28] In contrast, the threshold energies of the palladium cluster ions show a rather smooth increase; as for silver, the E_{TH} values clearly lie below the bulk work function.

Discussion

If the cluster is assumed to be a conducting sphere, a simple model may be used to describe electron detachment. In particular, for a negatively charged sphere, the electron affinity
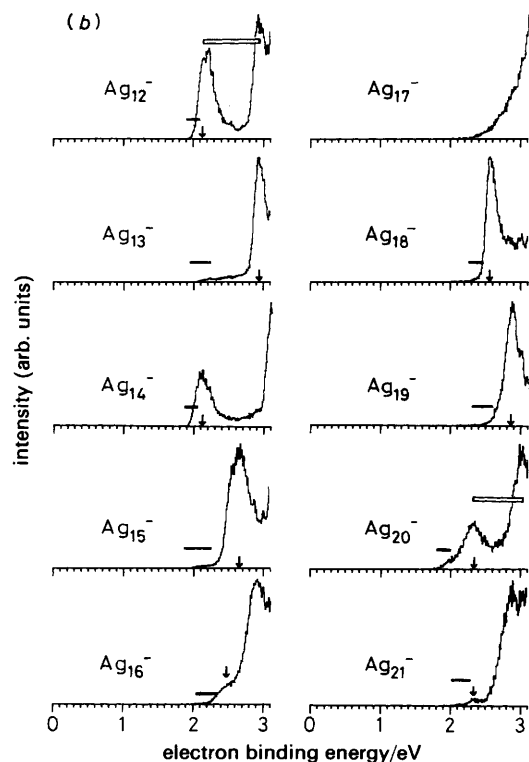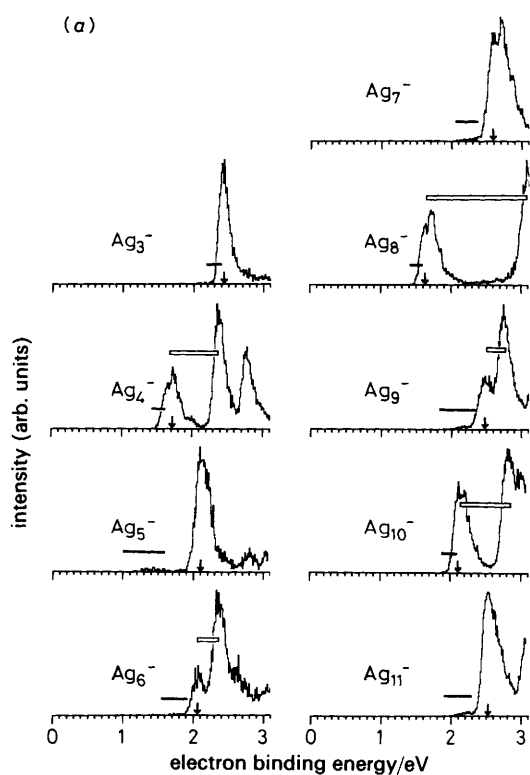
Fig. 3. (a) and (b) Photoelectron spectra of Ag$_n^-$ clusters (n = 3–21) at a detachment energy of 3.68 eV (337 nm). Each spectrum is an average over 10^4 shots. No background signal correction has been performed. Photoelectron thresholds (E_{TH}) as estimates of adiabatic electron affinities are marked by horizontal solid bars; the arrows indicate the positions of the first strong maxima (E_{MAX}). The open bars correspond to the gaps between the first and second strong maxima.
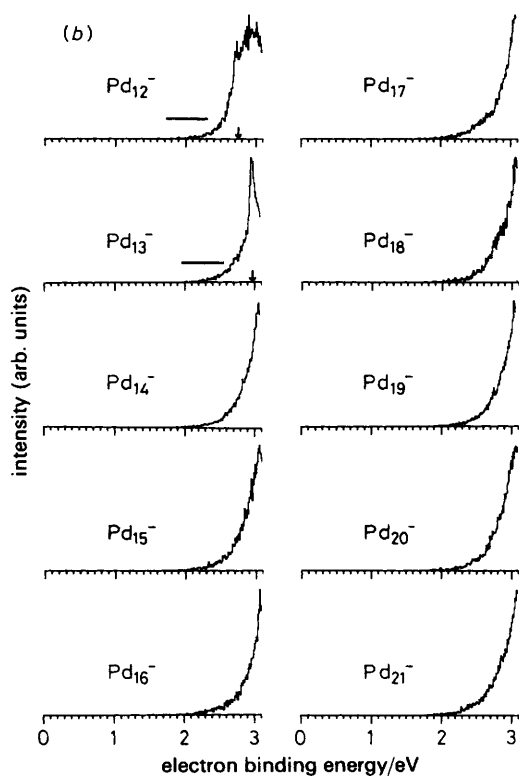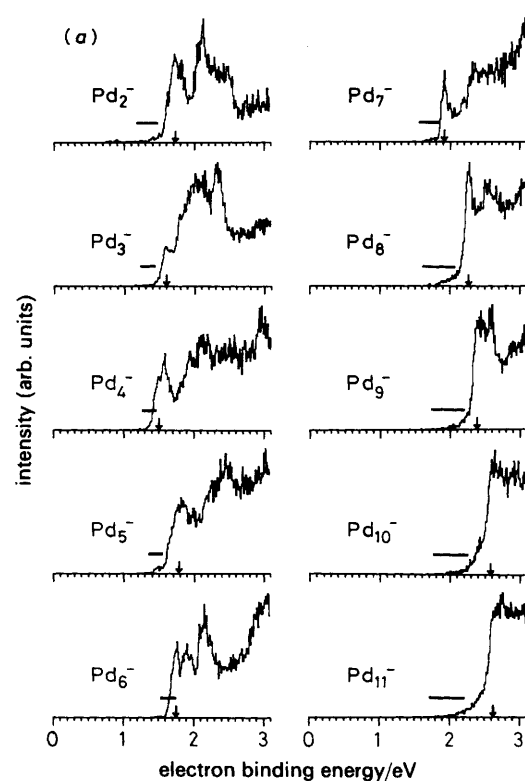
Fig. 4. (a) and (b) Photoelectron spectra of Pd$_n^-$ clusters (n = 2–21).
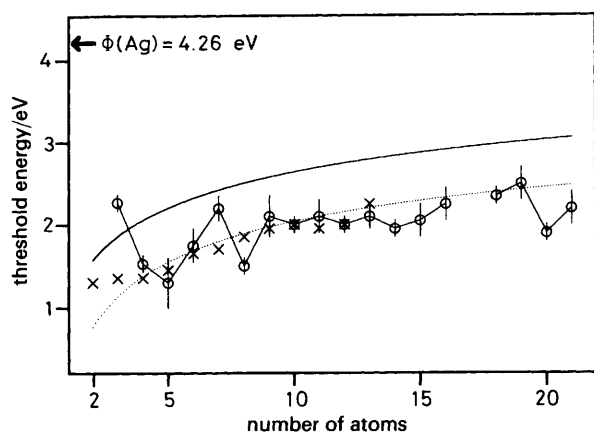
Fig. 5. Measured electron affinities E_{TH} as function of atom number. (○), Ag_n^-; (×), Pd_n^-. The classical behaviour as expected by the conducting sphere model [eqn (1)] yields the dotted line for Ag_n^- ($r_s = 1.65$ Å; $r_0 = 0.5$ Å) and the full line for Pd_n^- ($r_s = 1.52$ Å; $r_0 = 0.5$ Å).

$E_{ea}(R)$ as function of the sphere radius, R, is given by:[29]

$$E_{ea}(R) = \phi - \frac{5}{8}\frac{e^2}{R}.\qquad(1)$$

This relationship, and especially the factor 5/8, is currently the subject of controversy.[30-32] However, eqn (1) holds for a lot of ionization potential data of singly[33] and multiply charged[34] metal clusters and for electron affinities of group Ib and IIIa clusters.[12,18,22] For a comparison of the measured electron affinities with eqn (1) the cluster radius has to be determined. With the assumption of close atom packing, R is given by

$$R = r_s n^{1/3} + r_0\qquad(2)$$

where r_s is half the internuclear separation and r_0 is a parameter to account for the 'spilling out' of the electron charge beyond the boundary of the cluster.[12] Since neither r_s nor r_0 are accurately known, they may serve as fitting parameters, with $r_s = 80$–100% of the bulk internuclear separation and

Table 1. Photoelectron threshold energies E_{TH} (as estimates of upper bounds of adiabatic electron affinities) and positions of the first maxima E_{MAX} of silver and palladium cluster anions

	Ag_n^-		Pd_n^-	
n	E_{TH}/eV	E_{MAX}/eV	E_{TH}/eV	E_{MAX}/eV
2	1.0 ± 0.2	—	1.30 ± 0.15	1.71
3	2.27 ± 0.1	2.43	1.35 ± 0.1	1.60
4	1.53 ± 0.1	1.71	1.35 ± 0.1	1.50
5	1.30 ± 0.3	2.1	1.45 ± 0.1	1.78
6	$1.75^{+0.15}_{-0.2}$	2.05	1.65 ± 0.1	1.74
7	2.20 ± 0.15	2.6	1.70 ± 0.15	1.91
8	1.50 ± 0.1	1.62	1.85 ± 0.25	2.28
9	2.10 ± 0.25	2.48	1.95 ± 0.25	2.39
10	2.00 ± 0.1	2.1	2.00 ± 0.25	2.58
11	2.10 ± 0.2	2.51	1.95 ± 0.25	2.62
12	2.00 ± 0.1	2.12	2.00 ± 0.3	2.74
13	2.10 ± 0.15	2.94	2.25 ± 0.3	2.96
14	1.95 ± 0.1	2.12		
15	2.05 ± 0.2	2.65		
16	$2.25^{+0.1}_{-0.2}$	2.48		
17	—	—		
18	2.35 ± 0.1	2.56		
19	$2.50^{+0.1}_{-0.2}$	2.86		
20	1.90 ± 0.1	2.33		
21	$2.20^{+0.1}_{-0.2}$	2.32		

$r_0 = 0$–1 Å. Using $r_s = 1.65$ Å ($0.9r_{bulk}$) and $r_0 = 0.5$ Å, eqn (1) can be fitted reasonably well to the trend of the silver PE thresholds (fig. 5, dotted line). Apparently, the electron affinities of these small clusters follow roughly the electrostatic curve. A similar agreement is found for Cu_n^- [ref. (12)], Al_n^- [ref. (18)], In_n^- and Tl_n^- [ref. (35)].

Of course, this agreement should not be taken as proof of good electrical conductivity of the cluster. Indeed, the electron confinement to volumes less than 10 Å in diameter introduces discrete energy states, with separations of the order of 1 eV; these states are also reflected in the peak structure of the PE spectra. The behaviour as given by eqn (1) indicates rather high cluster polarizability. For example, a relationship similar to that of eqn (1) has recently also been found for $(H_2O)_n^-$ clusters,[36] where the excess electron is bound by a solvation sphere in a dielectric medium with a high static dielectric constant.

In contrast to Ag_n^- clusters, Pd_n^- photoelectron thresholds cannot satisfactorily be described by eqn (1), cf. the full line in fig. 5. A similar behaviour is observed for Ni_n^- thresholds.[22] Also other systems like Sn_n^- and Pb_n^- [ref. (37)] do not follow the classical picture.

These results are consistent with expectation: the valence electrons in Ag and Cu (having mainly s/p character in bulk metal) will be delocalized when atoms are brought together to form a cluster; such behaviour is also expected from calculations for lithium clusters.[10] In contrast, Pd and Ni are less sensitive to the spatial limitations of the cluster, and thus exhibit a weaker n dependence; in addition, their high multiplicity gives rise to a large density of states,[38] which again helps to wash out n-dependent characteristics. This argument is supported by a tight-binding type of electronic theory in which the d electrons are expected to contribute dominantly to the structure of transition metal clusters.[39] The s electrons are less localized and thus less structure sensitive as the electron hopping integral and effective coordination numbers are much larger for s than for d electrons. The high density of states near the Fermi level in Pd and Ni clusters strongly suppress possible shell structures.

Besides an overall increase of the photoelectron threshold with increasing n, fig. 5 shows fine structure in the n dependence for Ag_n^-. A pronounced even–odd behaviour and a minimum at Ag_8^- and Ag_{20}^- are superimposed on the classical curve. Similar alternations in, e.g. photoionization energies of alkali-metal[40,41] and copper clusters,[42] unimolecular decay rates and fragmentation cross-sections of copper clusters[21,43] and photofragmentation of alkali-metal[44] and silver clusters[45] have been observed.

Various quantum-chemical calculations for small alkali-metal and alkali-metal-like clusters show such even/odd oscillations in binding energies, ionization potentials, electron affinities, etc.[4,5,9,10,46] Very recently Bonačić-Koutecký et al.[20] performed ab initio calculations on small sodium clusters, yielding an explanation for Na_n^-, $n = 2$–5, photoelectron spectra.[19] Fig. 6 shows a comparison of our Ag_n^- and Cu_n^- photoelectron spectra (now taken at a detachment energy of $hv = 5.0$ eV) with the Na_n^- data of McHugh et al.[19] Several features of the silver and copper cluster PE spectra are also found in the sodium data, the absolute binding energy of Na_n^-, of course, being shifted to lower values. In addition, the lowest row gives calculations from ref. (20) yielding reasonable agreement with some Na_n^- PE features. The similarity between the alkali-metal and alkali-metal-like cluster PE spectra gives rise to hope that a quantitative understanding of excited neutral cluster states will be developed one day even on the level of ab initio calculations.

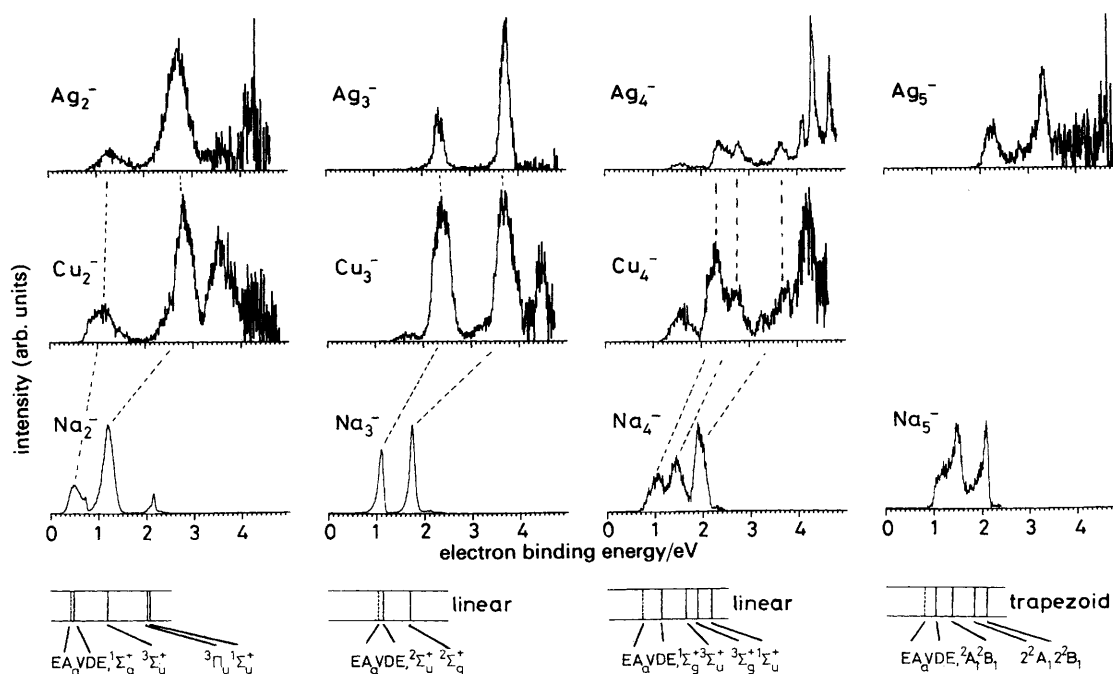For larger clusters different approaches to the jellium model reproduce strong discontinuities or also even–odd

Ag$_2^-$ Ag$_3^-$ Ag$_4^-$ Ag$_5^-$

intensity (arb. units)

Cu$_2^-$ Cu$_3^-$ Cu$_4^-$

Na$_2^-$ Na$_3^-$ Na$_4^-$ Na$_5^-$

0 1 2 3 4   0 1 2 3 4   0 1 2 3 4   0 1 2 3 4

electron binding energy/eV

linear   linear   trapezoid

EA$_a$,VDE,$^1\Sigma_g^+$ $^3\Sigma_u^+$ $^3\Pi_u$ $^1\Sigma_u^+$ EA$_a$,VDE,$^2\Sigma_u^+$ $^2\Sigma_g^+$ EA$_a$,VDE,$^1\Sigma_g^+$$^3\Sigma_u^+$ $^3\Sigma_g^+$$^1\Sigma_u^+$ EA$_a$,VDE,^{2}A$_1^2$B$_1$ 2^2A$_1$,2^2B$_1$

Fig. 6. Direct comparison of Cu$_n^-$ and Ag$_n^-$ photoelectron spectra, now taken at a detachment energy of 5.0 eV, to Na$_n^-$ PE spectra of McHugh et al.[19] Features belonging to the same transitions (under the assumption of a roughly constant binding energy ratio) are connected by dashed lines. In addition, selected results of ab initio calculations of Bonačić-Koutecký et al.[20] are given on the bottom row.

variations of alkali-metal-like clusters.[1-3,47] The success of the jellium model as well as the close correspondence between the Ag$_n^-$ and Cu$_n^-$ cluster PE spectra (fig. 6) tempts us to try an explanation of some prominent features on the basis of the shell model.

First, we expect the first major shell closing at $n = 7$ with $(1s)^2(1p)^6$ having 8 electrons. This is indeed observed: the most weakly bound prominent state in Ag$_7^-$ as well as Cu$_7^-$ has a comparatively high binding energy. In the next largest cluster, $n = 8$, an additional occupied state with quite low binding energy appears to be added; this one might interpret as (1d). The corresponding Ag$_8^-$ PE spectrum (see fig. 3) shows a peak at 1.6 eV followed by a gap of more than 1 eV until the first excited neutral state is reached. This is the highest excitation energy we observed for most of the metal clusters. Only Pb$_4$ has a higher excitation energy [1.4 eV, cf. ref. (37)]. The next shell closing within the spherical jellium model is expected at $n = 18$ (1d). It should not be very prominent as the next shell (2s) closes at $n = 20$. Indeed, we again find a low-lying peak for Ag$_{20}^-$, followed by a region of low intensity, see fig. 3.

This admittedly rather qualitative success is encouraging enough to apply the jellium model to the finer details of the Ag (and Cu) cluster PE spectra. To this end we have to include non-spherical deformations into the effective cluster potential, e.g. by a modified Nilsson potential[47,48] or by self-consistent jellium calculations.[2] Such deformations already result in a qualitative reproduction of the even–odd alternations of ionization potentials[48] and electron affinities.[13] Of course, the jellium model neglects electron-core interaction and the fine structure of the potential due to the presence of individual atoms. Nevertheless, a rough understanding of some features of the PE spectra may be gained from the model, although a number of points remain unexplained. For example, the even–odd oscillation is broken at Ag$_{16}^-$ where the low-energy peak in the PE spectrum is missing; the origin of the flat thresholds is not clear. The latter may possibly be caused by localized components of the valence electrons, or a lower symmetry than assumed in the simple deformed jellium potential. These flat threshold features (cf. for example, Ag$_5^-$

and Ag$_{13}^-$) tend to weaken the strong even–odd alternation as is evident when comparing, e.g., the PE spectra of Ag$_{12}^-$, Ag$_{13}^-$ and Ag$_{14}^-$. The deformed jellium model tends more to the n dependence of E_{MAX} rather than that of E_{TH}. E_{TH} varies relatively smoothly with n and is, therefore, better described by the classical model [eqn (1)].

Nevertheless, we regard the jellium model as being a powerful tool especially for the understanding of large clusters. An extention is urgently needed (taking into consideration the presence of individual atoms) to electronically excited cluster states in the geometry of the anion.

PE spectra of palladium anions have completely different shapes and n dependences as shown in fig. 4. No distinct band gaps are observed, nor is there any dramatic change in the positions of the threshold and first maximum energies. This is consistent with the behaviour of E_{TH} discussed earlier which increases gradually with n and slowly approaches an electron binding energy of ca. 2 eV (still far away from the work function value of bulk polycrystalline palladium of 5.12 eV).[28] This can be attributed to the more localized d electrons in Pd, which also dominate the density of states near the Fermi level in the bulk. The Pd cluster PE spectra already resemble those of bulk palladium.[49] A similar high density of states is observed in Ni$_n^-$ PE spectra[22,50] which also display no distinct gaps or pronounced discontinuities of E_{TH} in accordance with calculation.[38] Thus the differences in the fundamental roles of the delocalized s/p electrons in bulk Ag on the one hand, and the more localized d electrons in Pd on the other, remain apparent down to the rather small aggregates which have been studied here.

Conclusion

We have presented PE spectra of mass-separated Ag$_n^-$ and Pd$_n^-$ cluster anions which give information about the density of states a few eV beyond the photodetachment thresholds. In the case of Ag$_n^-$ the main contribution stems from delocalized atomic s/p orbitals which appear to follow, in part, the jellium model. A strong similarity between Ag$_n^-$ and Cu$_n^-$ PE spectra is demonstrated. In addition, several features of Ag$_n^-$

and Cu_n^- are similar to those of sodium cluster anions.[19] For Na_n^-, $n = 2-5$, recent *ab initio* calculations of Bonačić-Koutecký *et al.* have yielded the energetic positions and assignments of electronically excited states which we also compare with Ag_n^- and Cu_n^-.

Pd_n^- PE spectra show a high density of states; the PE thresholds as well as the intensity profiles cannot be explained by the jellium model. The density of states near the Fermi level in the bulk is mainly produced by localized d electrons. Since localized states are less affected by confinement in the volume of a cluster, one can expect some similarity between the cluster PE spectra and those of the bulk even at small cluster sizes. Although there is no simple explanation for the observed spectral features, they are expected to reflect to a larger extent the actual geometrical structure of the cluster. In contrast, in the case of Ag one might suspect that the geometrical structure has less influence on the spectral features near the Fermi level.

References

1 J. L. Martins, R. Car and J. Buttet, *Surf. Sci.*, 1981, **106**, 265.
2 W. Ekardt, *Phys. Rev. B*, 1984, **29**, 1558; W. Ekardt and Z. Penzar, *Phys. Rev. B*, 1988, **38**, 4273; W. Ekardt and Z. Penzar, personal communication.
3 W. A. Knight, K. Clemenger, W. A. de Heer, W. Saunders, M. Y. Chou and M. L. Cohen, *Phys. Rev. Lett.*, 1984, **52**, 2141.
4 R. C. Baetzold, *J. Chem. Phys.*, 1978, **68**, 555.
5 J. Flad, G. Igel-Mann, H. Preuss and H. Stoll, *Chem. Phys.*, 1984, **90**, 257.
6 K. Raghavachari, V. Logovinsky, *Phys. Rev. Lett.*, 1985, **55**, 2853.
7 T. H. Upton, *Phys. Rev. Lett.*, 1986, **56**, 2168.
8 L. C. Balbas, A. Rubio, J. A. Alonso and G. Borstel, *Chem. Phys.*, 1988, **120**, 239.
9 V. Bonačić-Koutecký, P. Fantucci, G. Koutecký, *Phys. Rev. B*, 1988, **37**, 4369.
10 I. Boustani, W. Pewerstorf, G. Koutecký, P. Fantucci, V. Bonačić-Koutecký and J. Koutecký, *Phys. Rev. B*, 1987, **18**, 9437.
11 T. P. Martin and B. Wassermann, *J. Chem. Phys.*, 1989, **90**, 5108.
12 D. G. Leopold, J. H. Ho and W. C. Lineberger, *J. Chem. Phys.*, 1987, **86**, 1715.
13 O. Cheshnovsky, P. J. Brucat, S. Yang, C. L. Pettiette, M. J. Craycraft and R. E. Smalley, in *Physics and Chemistry of Small Clusters*, NATO ASI Ser. B, 1987, vol. 158, 1; C. L. Pettiette, S. H. Yang, M. J. Craycraft, J. Conceicao, R. T. Laaksonen, O. Cheshnovsky and R. E. Smalley, *J. Chem. Phys.*, 1988, **88**, 5377.
14 K. Rademann, B. Kaiser, U. Even and F. Hensel, *Phys. Rev. Lett.*, 1987, **59**, 2319.
15 M. J. Deluca, B. Niu and M. A. Johnson, *J. Chem. Phys.*, 1988, **88**, 5857.
16 J. V. Coe, J. T. Snodgrass, C. B. Freidhoff, K. M. McHugh and K. H. Bowen, *Chem. Phys. Lett.*, 1986, **124**, 274.
17 G. Ganteför, K. H. Meiwes-Broer and H. O. Lutz, *Phys. Rev. A*, 1988, **37**, 2716.
18 G. Ganteför, M. Gausa, K. H. Meiwes-Broer and H. O. Lutz, *Z. Phys. D*, 1988, **9**, 253.
19 K. M. McHugh, J. G. Eaton, G. H. Lee, H. W. Sarkas, L. H. Kidder, J. T. Snodgrass, M. R. Manaa and K. H. Bowen, *J. Chem. Phys.*, 1989, **91**, 3792.
20 V. Bonačić-Koutecký, P. Fantucci and J. Koutecký, *J. Chem. Phys.*, 1989, **91**, 3794.
21 W. Begemann, S. Dreihöfer, G. Ganteför, H. R. Siekmann, K. H. Meiwes-Broer and H. O. Lutz, in *Elemental and Molecular Clusters*, Springer Series on Materials Science, (Springer-Verlag, Berlin, 1988), vol. 6, p. 230.
22 G. Ganteför, M. Gausa, K. H. Meiwes-Broer and H. O. Lutz, *Faraday Discuss. Chem. Soc.*, 1988, **86**, 197.
23 V. E. Bondybey and J. H. English, *J. Chem. Phys.*, 1981, **74**, 6978.
24 T. G. Dietz, M. A. Duncan, D. E. Powers and R. E. Smalley, *J. Chem. Phys.*, 1981, **74**, 6511.
25 P. Kruit and F. H. Read, *J. Phys. E*, 1983, **16**, 313.
26 H. Hotop and W. C. Lineberger, *J. Phys. Chem. Ref. Data*, 1975, **4**, 539.
27 J. Bernholc and J. C. Phillips, *Phys. Rev. B*, 1986, **33**, 7395.
28 *Handbook of Chemistry and Physics*, ed. R. C. Weast (CRC Press, Boca Raton, 1978).
29 D. M. Wood, *Phys. Rev. Lett.*, 1981, **46**, 749.
30 J. P. Perdew, *Phys. Rev. B*, 1988, **37**, 6175.
31 G. Makov, A. Nitzan and L. E. Brus, *J. Chem. Phys.*, 1988, **88**, 5076.
32 H. Haberland, to be published.
33 E. Schumacher and M. Kappes, in *Large Finite Systems*, Proc. of the 20th Jerusalem Symp. on Quantum Chemistry and Biochemistry, ed. J. Jortner, A. Pullman and B. Pullman, (D. Reidel, Dortrecht, 1987), p. 289.
34 C. Bréchignac, Ph. Cahuzac, F. Carlier, M. de Frutos and J. Leygnier, *J. Chem. Soc., Faraday Trans.*, 1990, **86**, 2525.
35 M. Gausa, G. Ganteför, K. H. Meiwes-Broer and H. O. Lutz, *Int. J. Mass. Spectrom. Ion Process.*, in press.
36 R. N. Barnett, U. Landman, C. L. Cleveland, N. R. Kestner and J. Jortner, *Chem. Phys. Lett.*, 1988, **148**, 249.
37 G. Ganteför, M. Gausa, K. H. Meiwes-Broer and H. O. Lutz, *Z. Phys. D*, 1989, **12**, 405.
38 I. Shim, K. A. Gingerich, in *The physics and chemistry of small clusters*, NATO ASI Ser. B, 1987, **158**, 523.
39 G. M. Pastor, J. Dorantes-Dávila and K. H. Bennemann, *Chem. Phys. Lett.*, 1988, **148**, 459.
40 M. M. Kappes, M. Schär, U. Röthlisberger, C. Yeretzian and E. Schumacher, *Chem. Phys. Lett.*, 1988, **143**, 251.
41 H. G. Limberger and T. P. Martin, *J. Chem. Phys.*, 1989, **90**, 2979.
42 D. E. Powers, S. G. Hansen, M. E. Geusic, D. L. Michalopoulos and R. E. Smalley, *J. Chem. Phys.*, 1983, **78**, 2866.
43 W. Begemann, S. Dreihöfer, K. H. Meiwes-Broer and H. O. Lutz, *Z. Phys. D*, 1986, **3**, 183.
44 C. Bréchignac, Ph. Cahuzac, J-Ph. Roux, D. Pavolini and F. Spiegelmann, *J. Chem. Phys.*, 1987, **87**, 5694; C. Bréchignac and Ph. Cahuzac, *Chem. Phys. Lett.*, 1985, **117**, 365.
45 P. Fayet and L. Wöste, *Z. Phys. D*, 1986, **3**, 177.
46 P. Jena, S. N. Khanna and B. K. Rao, in *Microclusters*, Springer Series in Materials Science 4, (Springer-Verlag, Berlin, 1987).
47 K. Clemenger, *Phys. Rev. B*, 1985, **32**, 1359.
48 W. A. Saunders, Thesis (Berkeley, 1986).
49 A. Y. C. Yu and W. E. Spicer, *Phys. Rev.*, 1968, **169**, 729.
50 K. M. Ervin, J. Ho and W. C. Lineberger, *J. Chem. Phys.*, 1988, **89**, 4514.